J. Am. Chem. Soc. 1983, 105, 2625-2632

Control of Spin State in (Porphinato)iron(III) Complexes. An Axial Ligand Orientation Effect Leading to an Intermediate-Spin Complex. Molecular Structure and Physical Characterization of the Monoclinic Form of Bis(3-chloropyridine)(octaethylporphinato)iron(III) Perchlorate

W. Robert Scheidt,*[1] David K. Geiger,[1] Robert G. Hayes,[1] and George Lang*[2]

Contribution from the Department of Chemistry, University of Notre Dame, Notre Dame, Indiana 46556, and the Department of Physics, Pennsylvania State University, University Park, Pennsylvania 16802. Received July 20, 1982

Abstract: The iron(III) porphyrinate $[Fe(OEP)(3\text{-}Clpy)_2]ClO_4$, which has been previously reported as exhibiting a thermal spin equilibrium ($S = {}^1/_2 \rightleftharpoons S = {}^5/_2$), is shown to have even more complex magnetic properties. A quantum-admixed intermediate-spin state can also exist for this molecule and is apparently stabilized by solid-state effects. This new admixed intermediate-spin state crystallizes in the monoclinic crystal system unlike the thermal spin equilibrium system which crystallizes[10] in the triclinic system. This new phase has been characterized by magnetic susceptibilities, Mössbauer spectra, electron paramagnetic resonance, and a crystal structure determination. All physical data, including a Mössbauer quadrupole splitting of 2.7 mm/s, a near axial EPR spectrum with $g_\perp$ of 4.9, and a magnetic moment of 4.7 μ_B at 295 K, and the molecular structure are consistent with the assignment of a quantum-admixed intermediate-spin state. Crystal data: monoclinic, space group $P2_1/a$, $a = 20.779$ (7) Å, $b = 19.886$ (5) Å, $c = 22.142$ (6) Å, and $\beta = 101.18$ (2)°, and $Z = 8$. The structure is based on 11 169 observed reflections measured on an automated diffractometer. Pertinent structural parameters include relatively short equatorial Fe–N_p bond distances of 2.005 (6) Å and long axial bond distances of 2.310 (17) Å. The structures of the two crystallographically independent $[Fe(OEP)(3\text{-}Clpy)_2]^+$ ions are essentially identical.

A particularly notable feature of the hemoproteins is the near commonality of the heme prosthetic group (iron derivatives of protoporphyrin IX) despite their impressively varied chemical functions. The recurrence of the same iron porphyrinate active site in the hemoproteins leads to the notion that a particular physiological function is achieved by protein fine tuning of the structure around the heme. Both the axial ligation to the heme group and the nature of the immediate environment are critical in controlling the physical and chemical properties of the iron atom. The magnetic properties of the heme prosthetic groups have been much studied. Thermal spin equilibria between a low-spin and a high-spin state for the iron(III) atom in the ferric hemoproteins are well-known.[3] A somewhat surprising aspect of these equilibria is the quantitative differences between various hemoproteins even when the same axial ligands are present. Phenomena such as these increase interest in understanding precisely how the protein structure influences the electronic structure of its prosthetic group.

In isolated iron porphyrinate complexes, the modulation of axial ligation provides primary control of spin state.[4] For example, in six-coordinate iron(III) species, the coordination of strong field ligands leads to low-spin ($S = {}^1/_2$) complexes, e.g., bis(imidazole)iron(III) derivatives.[5] Weaker field ligands, e.g., water,[6] or sulfoxides,[7] lead to high-spin six-coordinate complexes with radially expanded cores. Still weaker field ligands, e.g., tricyanomethanide,[8] lead to intermediate ($S = {}^3/_2$) or admixed intermediate-spin derivatives. With the appropriate choice of axial ligands, it is also possible to prepare[9] complexes in a thermal spin equilibrium between the high-spin ($S = {}^5/_2$) and low-spin ($S = {}^1/_2$) states. We have recently structurally characterized[10] one such derivative, bis(3-chloropyridine)(octaethylporphinato)iron(III) perchlorate, $[Fe(OEP)(3\text{-}Clpy)_2]ClO_4$,[11] at 98 K (low-spin) and at 293 K (thermal spin mixture). For the thermal spin mixture, we were able to accomplish the crystallographic resolution of the structure of the two spin isomers.

In the course of those investigations, we isolated a second crystalline form of $[Fe(OEP)(3\text{-}Clpy)_2]ClO_4$. The lattices of both forms, the triclinic form reported previously[10] and the new monoclinic form, contain *only* $[Fe(OEP)(3\text{-}Clpy)_2]^+$ cations and its associated perchlorate anion. Temperature-dependent magnetic susceptibilities for the two crystalline forms were decidedly different. The triclinic form has values consistent with a thermal spin equilibrium.[9a,12] Magnetic moments of the monoclinic form were significantly higher. Solution susceptibilities (methylene chloride solution) of both crystalline forms were identical. In order to understand these differing susceptibilities, we have now carried out a structural analysis of the monoclinic form. This analysis and other physical characterization, most notably Mossbauer studies, suggest that the ground state of the monoclinic form is a quantum-admixed intermediate-spin state.[13] The differing electronic structures of the two crystalline forms of $[Fe(OEP)(3\text{-}Clpy)_2]ClO_4$ appear to result from well-defined differences in

---

(1) University of Notre Dame.

(2) Pennsylvania State University.

(3) Beetlestone, J.; George, P. *Biochemistry* **1964**, *3*, 707–714. Iizuka, T.; Kotani, M. *Biochim. Biophys. Acta* **1968**, *154*, 417–419; *Ibid.* **1969**, *181*, 275–286; *Ibid.* **1969**, *194*, 351–363. Anusiem, A. C. I.; Kelleher, M. *Biopolymers* **1978**, *17*, 2047–2055. Perutz, M. F.; Sanders, J. K. M.; Chenerv, D. H.; Noble, R. W.; Pennelly, R. R.; Fund, L. W.-M.; Ho, C.; Giannini, I.; Porschke, D.; Winkler, H. *Biochemistry* **1978**, *17*, 3640–3652. Messana, C.; Cerdonio, M.; Shenkin, P.; Noble, R. W.; Fermi, G.; Perutz, R. W.; Perutz, M. F. *Ibid.* **1978**, *17*, 3652–3662. Sligar, S. G. *Ibid.* **1976**, *15*, 5399–5406. Lange, R.; Bonfils, C.; Debye, P. *Eur. J. Biochem.* **1977**, *79*, 623–628. Yonetani, T.; Iizuka, T.; Asakura, T. *J. Biol. Chem.* **1972**, *247*, 863–868.

(4) Scheidt, W. R.; Reed, C. A. *Chem. Rev.* **1981**, *81*, 543–555.

(5) Collins, D. M.; Countryman, R.; Hoard, J. L. *J. Am. Chem. Soc.* **1972**, *94*, 2066–2072.

(6) Scheidt, W. R.; Cohen, I. A.; Kastner, M. E. *Biochemistry* **1979**, *18*, 3546–3552.

(7) Mashiko, T.; Kastner, M. E.; Spartalian, K.; Scheidt, W. R.; Reed, C. A. *J. Am. Chem. Soc.* **1978**, *100*, 6354–6362.

(8) Summerville, D. A.; Cohen, I. A.; Hatano, K.; Scheidt, W. R. *Inorg. Chem.* **1978**, *17*, 2906–2910.

(9) (a) Hill, H. A. O.; Skyte, P. D.; Buchler, J. W.; Leuken, H.; Tonn, M.; Gregson, A. K.; Pellizer, G. *J. Chem. Soc., Chem. Commun.* **1979**, 151–152. (b) Kassner, R. J.; Huang, Y.-P. *J. Am. Chem. Soc.* **1979**, *101*, 5807–5810. (c) Collman, J. P.; Sorell, T. N.; Hodgson, K. O.; Kulshrestha, A. K.; Strouse, C. E. *J. Am. Chem. Soc.* **1978**, *99*, 5180–5181.

(10) Scheidt, W. R.; Geiger, D. K.; Haller, K. J. *J. Am. Chem. Soc.* **1982**, *104*, 495–499.

(11) Abbreviations used: OEP, dianion of octaethylporphyrin; 3-Clpy, 3-chloropyridine; N_p, porphinato nitrogen atom; Ct, center of porphinato core.

(12) Gregson, A. K. *Inorg. Chem.* **1981**, *20*, 81–87.

(13) Maltempo, M. M.; Moss, T. H. *Q. Rev. Biophys.* **1976**, *9*, 181–215.

0002-7863/83/1505-2625$01.50/0

Table I. Summary of Crystal Data and Intensity Collection Parameters for $[Fe(OEP)(3\text{-}Clpy)_2]ClO_4$

formula	$FeCl_3O_4N_6C_{46}H_{52}$
M_r, amu	915.2
cryst dimensns, mm	0.6 × 0 5 × 0.3
space group	$P2_1/a$
temp, K	293
a, Å	20.779 (7)
b, Å	19.886 (5)
c, Å	22.142 (6)
β, deg	101.18 (2)
V, Å^3	8975.9
Z	8
calcd density, g/cm^3	1.354
obsd density, g/cm^3	1.34
radiation	graphite monochromated Mo Kα ($\lambda = 0.71073$ Å)
scan technique	θ–2θ
scan range	0.5° below Kα_1, to 0.5° above Kα_2
scan rate, deg/min	2–24
background	profile analysis
2θ limits	3.5–54.9
criterion for observatn	$F_o > 3\sigma(F_o)$
unique obsd data	11169
μ, mm^{-1}	0.562
R_1	0.087
R_2	0.094
goodness of fit	1.976

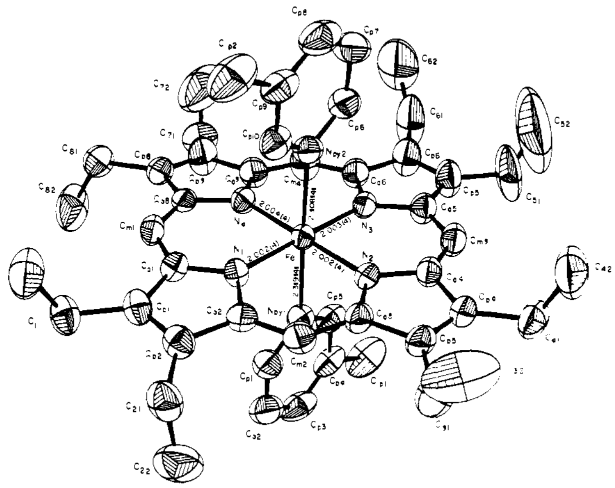

Figure 1. Computer-drawn model of molecule one of *mono*-[Fe(OEP)(3-Clpy)$_2$]ClO$_4$. The labeling scheme for the atoms is given. Bond distances in the coordination group are shown. Ellipsoids are contoured to enclose 50% of the electron density. For possible comparison, the same relative orientation of the molecule as that used in ref 10 is given.

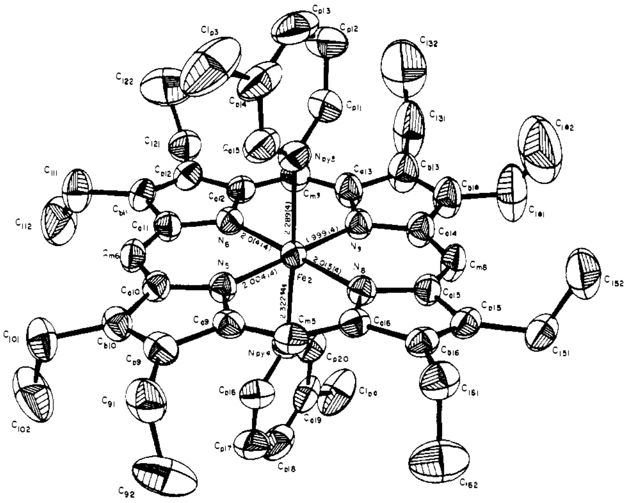

Figure 2. Computer-drawn model for molecule two of *mono*-[Fe(OEP)(3-Clpy)$_2$]ClO$_4$. The same information presented in Figure 1 is given here.

axial ligand orientations. We report our characterization of the monoclinic form of [Fe(OEP)(3-Clpy)$_2$]ClO$_4$ herein.

Experimental Section

Synthesis. [Fe(OEP)(3-Clpy)$_2$]ClO$_4$ was synthesized as described previously.[10] Single crystals were grown by slow vapor diffusion of hexane into 1:10 3-chloropyridine/chloroform solutions of [Fe(OEP)(3-Clpy)$_2$]ClO$_4$ (saturated, approximately 17 mg/mL). Both the previously described triclinic crystals and the present monoclinic phase of the compound were obtained in this fashion. The factors that lead to the isolation of one crystalline phase or the other are not presently understood. On the basis of optical and X-ray examination it appears that only one particular phase was obtained in any given crystal preparation. All physical measurements reported herein were derived from crystals of known crystalline modification; the phase of at least two crystals of any given batch were identified by X-ray diffraction methods. Mossbauer spectra were obtained on crushed crystalline specimens as described previously.[7]

Magnetic Data. Magnetic susceptibilities in the solid state were measured on a Faraday balance as described previously[10] and were corrected for diamagnetism. Effective magnetic moments observed for the monoclinic phase are 77 K, 3.7 μ_B; 103 K, 3.8 μ_B; 126 K, 3.9 μ_B; 177 K, 4.2 μ_B; 295 K, 4.7 μ_B. Values previously reported for the triclinic phase are 77 K, 2.7 μ_B; 100 K, 2.9 μ_B; 110 K, 3.0 μ_B; 133 K, 3.1 μ_b; 170 K, 3.3 μ_B; 294 K, 4.7 μ_B. The moments for the monoclinic phase are seen to be significantly larger, although the two phases appear to give identical moments in solution (methylene chloride solution, 4.6 μ_B, 313 K).

Preliminary X-ray Examination and Data Collection. Preliminary examination of crystals of monoclinic [Fe(OEP)(3-Clpy)$_2$]ClO$_4$ on a Nicolet P$\bar{1}$ automated diffractometer established an eight-molecule unit cell, space group $P2_1/a$. There are thus two complete molecules of [Fe(OEP)(3-Clpy)$_2$]ClO$_4$ in the asymmetric unit of structure. Attempts to measure cell constants and intensity data at temperatures below room temperature were frustrated by visible fracturing of single-crystal specimens at temperatures only 20–40 deg below ambient. Reexamination of the resulting crystal fragments at room temperature did not reveal a phase change. Consequently all subsequent measurements were obtained at the ambient laboratory temperature of 293 K.

A single-crystal specimen with dimensions of 0.6 × 0.5 × 0.3 mm was used for data collection and cell constant determination. Least-squares refinement of the setting angles of 60 automatically centered reflections with $24 < 2\theta < 38°$ led to the cell constants reported in Table I. Details of the intensity data collection parameters are also found in Table I. Intensity data were reduced to relative structure factors as described previously.[14]

Structure Solution and Refinement. The structure was solved in the space group $P2_1/a$, using the direct methods program MULTAN78.[15] The resulting E map gave positions of both iron atoms, all atoms of the two porphinato ligands, and atoms of three of the four 3-chloropyridine ligands in the asymmetric unit. The positions of the remaining atoms were found in subsequent difference Fourier syntheses. One of the perchlorate anions was found to be disordered by a 60° rotation around the Cl_2–O_{22} vector. The two sets of disordered oxygen atoms were assigned occupancy factors of 0.6 and 0.4. After several cycles of least-squares refinement, difference Fourier maps revealed the positions of all the meso-hydrogen atoms and most of the hydrogen atoms associated with the ethyl groups and the 3-chloropyridine axial ligands. All hydrogen atoms were included in subsequent cycles of least-squares refinement as fixed, idealized contributors (C–H = 0.95 Å and B(H) = B(C) + 1.0 Å^2). Least-squares refinement was then carried to convergence for the 1108 parameters which included anisotropic temperature factors for all heavy atoms. At convergence, the final discrepancy indices were $R_1 = 0.087$ and $R_2 = 0.094$[16] with a final data/parameter ratio of 10.1. The highest peak in a final difference Fourier map was 0.48 e/Å^3 and was associated with

---

(14) Scheidt, W. R. *J. Am. Chem. Soc.* **1974**, *96*, 84–89.

(15) Programs used in this study included local modifications of Main, Hull, Lessinger, Germain, Declerq, and Woolfson's MLTAN78, Jacobson's ALFF and ALLS, Busing and Levy's ORFFE and ORFLS, and Johnson's ORTEP2. Atomic form factors were from Cromer and Mann (Cromer, D. T.; Mann, J. B. *Acta. Crystallogr., Sect. A* **1968**, *A24*, 321–323), with real and imaginary corrections for anomalous dispersion in the form factor of the iron and chlorine atoms from Cromer and Liberman (Cromer, D. T.; Liberman, D. J. *J. Chem. Phys.* **1970**, *53*, 1891–1898). Scattering factors for hydrogen were from Stewart et al. (Stewart, R. F.; Davidson, E. R.; Simpson, W. T. *Ibid.* **1965**, *42*, 3175–3187).

(16) $R_1 = \sum||F_o| - |F_c||/\sum|F_o|$ and $R_2 = [\sum w(|F_o| - |F_c|)^2/\sum w(F_o)^2]^{1/2}$

Table II. Fractional Atomic Coordinates[a]

A. molecule one				B. molecule two			
atom	*x*	*y*	*z*	atom	*x*	*y*	*z*
Fe(1)	0.99137(3)	0.36971(3)	0.24712(3)	Fe(2)	0.49336(3)	0.37341(3)	-0.25717(3)
Cl(p1)	1.05551(9)	0.10543(9)	0.15949(10)	Cl(p3)	0.41947(9)	0.09723(8)	-0.21198(10)
Cl(p2)	0.93784(9)	0.63961(8)	0.32923(9)	Cl(p4)	0.58107(9)	0.64125(9)	-0.31329(11)
Cl(1)	0.24378(8)	0.11751(10)	0.50106(7)	Cl(2)	0.23907(9)	0.36698(11)	-0.00392(8)
N(1)	1.0099(2)	0.3840(2)	0.3384(2)	N(5)	0.5001(2)	0.3499(2)	-0.1681(2)
N(2)	1.0799(2)	0.4061(2)	0.2419(2)	N(6)	0.5809(2)	0.3295(2)	-0.2562(2)
N(3)	0.9733(2)	0.3534(2)	0.1561(2)	N(7)	0.4863(2)	0.3976(2)	-0.3458(2)
N(4)	0.9029(2)	0.3327(2)	0.2522(2)	N(8)	0.4060(2)	0.4177(2)	-0.2577(2)
C(m1)	0.9062(2)	0.3463(2)	0.3617(2)	C(m5)	0.3946(2)	0.3932(3)	-0.1524(2)
C(m2)	1.1232(2)	0.4237(3)	0.3515(2)	C(m6)	0.6098(2)	0.2993(3)	-0.1476(2)
C(m3)	1.0742(3)	0.3982(3)	0.1312(2)	C(m7)	0.5870(2)	0.3431(3)	-0.3645(2)
C(m4)	0.8657(3)	0.3015(3)	0.1447(2)	C(m8)	0.3821(2)	0.4594(2)	-0.3635(2)
C(a1)	0.9698(2)	0.3695(2)	0.3796(2)	C(a9)	0.4554(3)	0.3639(3)	-0.1318(2)
C(a2)	1.0693(2)	0.4031(2)	0.3745(2)	C(a10)	0.5537(3)	0.3223(3)	-0.1295(2)
C(a3)	1.1288(2)	0.4255(2)	0.2908(2)	C(a11)	0.6226(2)	0.3015(3)	-0.2061(2)
C(a4)	1.1061(2)	0.4143(2)	0.1894(2)	C(a12)	0.6112(2)	0.3217(2)	-0.3055(2)
C(a5)	1.0122(2)	0.3701(3)	0.1146(2)	C(a13)	0.5284(2)	0.3773(2)	-0.3844(2)
C(a6)	0.9168(2)	0.3271(3)	0.1209(2)	C(a14)	0.4354(2)	0.4316(2)	-0.3832(2)
C(a7)	0.8572(2)	0.3046(3)	0.2047(2)	C(a15)	0.3677(2)	0.4528(2)	-0.3056(2)
C(a8)	0.8745(2)	0.3287(2)	0.3033(2)	C(a16)	0.3724(2)	0.4194(2)	-0.2096(2)
C(b1)	1.0039(3)	0.3781(2)	0.4416(2)	C(b9)	0.4810(3)	0.3468(3)	-0.0693(2)
C(b2)	1.0660(3)	0.3976(3)	0.4387(2)	C(b10)	0.5431(3)	0.3224(4)	-0.0673(2)
C(b3)	1.1863(2)	0.4456(3)	0.2676(2)	C(b11)	0.6804(2)	0.2751(3)	-0.2245(2)
C(b4)	1.1722(2)	0.4391(3)	0.2060(2)	C(b12)	0.6748(2)	0.2890(3)	-0.2851(2)
C(b5)	0.9794(3)	0.3542(3)	0.0530(2)	C(b13)	0.5023(2)	0.3976(2)	-0.4464(2)
C(b6)	0.9204(3)	0.3275(4)	0.0571(2)	C(b14)	0.4450(3)	0.4314(2)	-0.4461(2)
C(b7)	0.8009(3)	0.2829(4)	0.2279(3)	C(b15)	0.3097(2)	0.4788(2)	-0.2866(2)
C(b8)	0.8103(2)	0.2994(3)	0.2879(2)	C(b16)	0.3117(2)	0.4561(2)	-0.2286(2)
C(11)	0.9765(3)	0.3655(3)	0.4994(2)	C(91)	0.4462(4)	0.3562(5)	-0.0161(3)
C(12)	0.9486(3)	0.4277(3)	0.5226(3)	C(92)	0.4506(5)	0.4230(7)	0.0030(4)
C(21)	1.1233(3)	0.4061(3)	0.4903(2)	C(101)	0.5940(4)	0.3070(5)	-0.0117(3)
C(22)	1.1667(3)	0.3453(4)	0.4985(3)	C(102)	0.6397(4)	0.3657(7)	0.0062(4)
C(31)	1.2522(3)	0.4649(3)	0.3070(3)	C(111)	0.7359(3)	0.2387(3)	-0.1822(3)
C(32)	1.2662(4)	0.5349(4)	0.3087(4)	C(112)	0.7939(4)	0.2809(4)	-0.1649(4)
C(41)	1.2164(3)	0.4526(3)	0.1612(3)	C(121)	0.7219(3)	0.2732(3)	-0.3266(3)
C(42)	1.2090(4)	0.5190(4)	0.1331(4)	C(122)	0.7334(4)	0.2038(4)	-0.3383(4)
C(51)	1.0068(4)	0.3650(5)	-0.0037(3)	C(131)	0.5310(3)	0.3788(3)	-0.5013(2)
C(52)	0.9895(8)	0.4134(10)	-0.0356(5)	C(132)	0.5127(4)	0.3082(3)	-0.5222(3)
C(61)	0.8651(3)	0.3079(5)	0.0062(3)	C(141)	0.3963(3)	0.4582(3)	-0.4995(2)
C(62)	0.8122(4)	0.3596(7)	-0.0037(4)	C(142)	0.3398(4)	0.4110(4)	-0.5201(3)
C(71)	0.7434(4)	0.2289(4)	0.1880(3)	C(151)	0.2580(2)	0.5210(3)	-0.3248(2)
C(72)	0.7031(5)	0.2758(5)	0.1645(6)	C(152)	0.2038(3)	0.4823(3)	-0.3632(3)
C(81)	0.7654(3)	0.2882(3)	0.3320(3)	C(161)	0.2618(2)	0.4684(3)	-0.1888(2)
C(82)	0.7763(4)	0.2242(4)	0.3666(4)	C(162)	0.2755(4)	0.5294(4)	-0.1485(3)
N(py1)	1.0367(2)	0.2631(2)	0.2627(2)	N(py3)	0.4433(2)	0.2733(2)	-0.2880(2)
C(p1)	1.0656(3)	0.2414(3)	0.3184(2)	C(p11)	0.4135(3)	0.2623(3)	-0.3463(2)
C(p2)	1.0928(3)	0.1787(3)	0.3288(3)	C(p12)	0.3851(3)	0.2019(3)	-0.3666(3)
C(p3)	1.0898(3)	0.1355(3)	0.2796(3)	C(p13)	0.3874(3)	0.1500(3)	-0.3258(3)
C(p4)	1.0607(2)	0.1573(3)	0.2228(3)	C(p14)	0.4165(3)	0.1609(3)	-0.2662(3)
C(p5)	1.0346(2)	0.2211(3)	0.2153(3)	C(p15)	0.4441(2)	0.2224(3)	-0.2484(2)
N(py2)	0.9480(2)	0.4764(2)	0.2299(2)	N(py4)	0.5471(2)	0.4743(2)	-0.2290(2)
C(p6)	0.9205(3)	0.4975(3)	0.1728(3)	C(p16)	0.5775(3)	0.4867(3)	-0.1711(3)
C(p7)	0.8975(3)	0.5627(3)	0.1613(3)	C(p17)	0.6102(3)	0.5459(4)	-0.1534(3)
C(p8)	0.9032(3)	0.6070(3)	0.2094(3)	C(p18)	0.6109(3)	0.5948(3)	-0.1964(4)
C(p9)	0.9300(3)	0.5858(3)	0.2672(3)	C(p19)	0.5805(3)	0.5824(3)	-0.2566(3)
C(p10)	0.9516(2)	0.5201(3)	0.2759(2)	C(p20)	0.5495(3)	0.5219(3)	-0.2706(3)
O(11)	0.2958(3)	0.1506(4)	0.4859(3)	O(21)	0.2702(6)	0.3904(8)	-0.0478(7)
O(12)	0.2674(5)	0.0651(6)	0.5347(5)	O(22)	0.1819(3)	0.3977(5)	0.0019(3)
O(13)	0.2141(4)	0.1511(6)	0.5357(4)	O(23)	0.2845(4)	0.3625(6)	0.0488(4)
O(14)	0.1990(3)	0.0983(4)	0.4517(3)	O(24)	0.2169(7)	0.3016(8)	-0.0277(8)
				O(25)	0.2514(13)	0.3291(9)	0.0438(8)
				O(26)	0.2681(10)	0.4316(10)	0.0052(9)
				O(27)	0.2452(13)	0.3481(9)	0.9448(6)

[a] The estimated standard deviations of the least significant digits are given in parentheses.

a perchlorate anion. All other peaks were less than 0.4 e/Å^3. Final atomic positional parameters are listed in Table II along with their equivalent isotropic temperature factors. Table III, a listing of the final anisotropic temperature factors, Table IV, a listing of the fixed hydrogen atom positions, and a listing of the final observed and calculated structure amplitudes are available as supplementary material.

Results and Discussion

The structure of the two crystallographically independent [Fe(OEP)(3-Clpy)$_2$]$^+$ ions are shown in Figures 1 and 2. The two are designated, arbitrarily, molecule one and molecule two. The figures illustrate the labeling scheme for all atoms; these are used in all tables. Also shown in the figures are the bond distances in the coodination groups of both iron(III) atoms. It should be noted that the molecular structures of the two independent ions, including all significant conformational aspects, are quite similar. Listing of individual values of bond distances and angles are given in Tables V and VI, respectively.

One of the major goals of this investigation was to understand the basis for the apparently different magnetic properties of the two crystalline forms of [Fe(OEP)(3-Clpy)$_2$]ClO$_4$. The triclinic phase will be denoted as *tri*-[Fe(OEP)(3-Clpy)$_2$]ClO$_4$ and the monoclinic phase as *mono*-[Fe(OEP)(3-Clpy)$_2$]ClO$_4$; if no label is given, the monoclinic phase is implied. In *tri*-[Fe(OEP)(3-Clpy)$_2$]ClO$_4$, a crystallographic inversion center at the iron atom is required. Although this is not a crystallographically required symmetry element in *mono*-[Fe(OEP)(3-Clpy)$_2$]ClO$_4$, each molecule has approximate $\bar{1}$ symmetry. As can be seen from Figures 1 and 2, excepting the orientation of some of the peripheral ethyl groups, approximate inversion centers are found at the iron(III) atoms. Thus the planes of the 3-chloropyridine ligands, within each molecule, are almost parallel. A significant difference in molecular structure in the two crystalline forms is the orientation of the pyridine rings with respect to the porphyrin core; the apparent importance of this will be discussed subsequently.

There are also some important differences in the bond distances in the coordination group of the iron(III) atom. Averaged values for the equatorial Fe–N$_p$ and axial Fe–N(3-Clpy) bond distances in both crystalline forms are given in Table VII. Values for *mono*-[Fe(OEP)(3-Clpy)$_2$]ClO$_4$ are averaged over the two molecules. The average structure of *mono*-[Fe(OEP)(3-Clpy)$_2$]ClO$_4$ is seen to differ significantly from that found for *either* the low-spin or high-spin structures of *tri*-[Fe(OEP)(3-

Table V. Bond Distances in $[Fe(OEP)(3\text{-}Clpy)_2]ClO_4$ (Å)

A. molecule one				B. molecule two			
type	distance	type	distance	type	distance	type	distance
Fe_1-N_1	2.002 (4)	$C_{b5}-C_{b6}$	1.356 (7)	Fe_2-N_5	2.004 (4)	$C_{b13}-C_{b14}$	1.367 (7)
Fe_1-N_2	2.002 (4)	$C_{b7}-C_{b8}$	1.345 (7)	Fe_2-N_6	2.014 (4)	$C_{b15}-C_{b16}$	1.354 (6)
Fe_1-N_3	2.003 (4)	$C_{b1}-C_{11}$	1.519 (6)	Fe_2-N_7	1.999 (4)	$C_{b9}-C_{91}$	1.507 (8)
Fe_1-N_4	2.004 (4)	$C_{b2}-C_{21}$	1.491 (7)	Fe_2-N_8	2.015 (4)	$C_{b10}-C_{101}$	1.492 (8)
Fe_1-N_{py1}	2.319 (4)	$C_{b3}-C_{31}$	1.522 (7)	Fe_2-N_{py3}	2.284 (4)	$C_{b11}-C_{111}$	1.521 (7)
Fe_1-N_{py2}	2.308 (4)	$C_{b4}-C_{41}$	1.502 (7)	Fe_2-N_{py4}	2.322 (4)	$C_{b12}-C_{121}$	1.499 (7)
N_1-C_{a1}	1.382 (5)	$C_{b5}-C_{51}$	1.491 (8)	N_5-C_{a9}	1.370 (6)	$C_{b13}-C_{131}$	1.502 (6)
N_1-C_{a2}	1.388 (5)	$C_{b6}-C_{61}$	1.497 (8)	N_5-C_{a10}	1.380 (6)	$C_{b14}-C_{141}$	1.497 (7)
N_2-C_{a3}	1.388 (5)	$C_{b7}-C_{71}$	1.719 (10)	N_6-C_{a11}	1.387 (6)	$C_{b15}-C_{151}$	1.491 (6)
N_2-C_{a4}	1.383 (5)	$C_{b8}-C_{81}$	1.493 (7)	N_6-C_{a12}	1.371 (5)	$C_{b16}-C_{161}$	1.506 (6)
N_3-C_{a5}	1.377 (5)	$C_{11}-C_{12}$	1.498 (8)	N_7-C_{a13}	1.393 (5)	$C_{91}-C_{92}$	1.393 (13)
N_3-C_{a6}	1.381 (6)	$C_{21}-C_{22}$	1.498 (8)	N_7-C_{a14}	1.386 (6)	$C_{101}-C_{102}$	1.509 (15)
N_4-C_{a7}	1.389 (6)	$C_{31}-C_{32}$	1.423 (9)	N_8-C_{a15}	1.385 (5)	$C_{111}-C_{112}$	1.457 (9)
N_4-C_{a8}	1.375 (6)	$C_{41}-C_{42}$	1.456 (8)	N_8-C_{a16}	1.383 (5)	$C_{121}-C_{122}$	1.431 (9)
$C_{a1}-C_{m1}$	1.383 (6)	$C_{51}-C_{52}$	1.208 (18)	$C_{a9}-C_{m5}$	1.387 (7)	$C_{131}-C_{132}$	1.505 (8)
$C_{a2}-C_{m2}$	1.379 (6)	$C_{61}-C_{62}$	1.490 (13)	$C_{a10}-C_{m6}$	1.382 (7)	$C_{141}-C_{142}$	1.504 (9)
$C_{a3}-C_{m2}$	1.373 (6)	$C_{71}-C_{72}$	1.293 (10)	$C_{a11}-C_{m6}$	1.371 (6)	$C_{151}-C_{152}$	1.487 (8)
$C_{a4}-C_{m2}$	1.368 (7)	$C_{81}-C_{82}$	1.481 (8)	$C_{a12}-C_{m7}$	1.373 (6)	$C_{161}-C_{162}$	1.500 (8)
$C_{a5}-C_{m3}$	1.388 (7)	$N_{py1}-C_{p1}$	1.334 (6)	$C_{a13}-C_{m7}$	1.390 (6)	$N_{py3}-C_{p11}$	1.337 (6)
$C_{a6}-C_{m4}$	1.372 (7)	$N_{py1}-C_{p5}$	1.334 (6)	$C_{a14}-C_{m8}$	1.382 (6)	$N_{py3}-C_{p15}$	1.338 (6)
$C_{a7}-C_{m4}$	1.374 (7)	$N_{py2}-C_{p6}$	1.348 (6)	$C_{a15}-C_{m8}$	1.378 (6)	$N_{py4}-C_{p16}$	1.339 (6)
$C_{a8}-C_{m1}$	1.378 (6)	$N_{py2}-C_{p10}$	1.331 (6)	$C_{a16}-C_{m5}$	1.364 (6)	$N_{py4}-C_{p20}$	1.328 (6)
$C_{a1}-C_{b1}$	1.428 (6)	$C_{p1}-C_{p2}$	1.389 (8)	$C_{a9}-C_{b9}$	1.424 (7)	$C_{p11}-C_{p12}$	1.375 (7)
$C_{a2}-C_{b2}$	1.440 (6)	$C_{p2}-C_{p3}$	1.370 (8)	$C_{a10}-C_{b10}$	1.436 (7)	$C_{p12}-C_{p13}$	1.366 (8)
$C_{a3}-C_{b3}$	1.444 (6)	$C_{p3}-C_{p4}$	1.361 (8)	$C_{a11}-C_{b11}$	1.439 (6)	$C_{p13}-C_{p14}$	1.359 (8)
$C_{a4}-C_{b4}$	1.440 (6)	$C_{p4}-C_{p5}$	1.382 (7)	$C_{a12}-C_{b12}$	1.463 (6)	$C_{p14}-C_{p15}$	1.375 (7)
$C_{a5}-C_{b5}$	1.435 (6)	$C_{p6}-C_{p7}$	1.389 (8)	$C_{a13}-C_{b13}$	1.433 (6)	$C_{p16}-C_{p17}$	1.378 (8)
$C_{a6}-C_{b6}$	1.428 (7)	$C_{p7}-C_{p8}$	1.370 (8)	$C_{a14}-C_{b14}$	1.445 (6)	$C_{p17}-C_{p18}$	1.364 (9)
$C_{a7}-C_{b7}$	1.434 (7)	$C_{p8}-C_{p9}$	1.361 (8)	$C_{a15}-C_{b15}$	1.447 (6)	$C_{p18}-C_{p19}$	1.381 (9)
$C_{a8}-C_{b8}$	1.434 (6)	$C_{p9}-C_{p10}$	1.382 (7)	$C_{a16}-C_{b16}$	1.448 (6)	$C_{p19}-C_{p20}$	1.372 (7)
$C_{b1}-C_{b2}$	1.361 (7)	$C_{p4}-Cl_{p1}$	1.728 (6)	$C_{b9}-C_{b10}$	1.370 (7)	$C_{p14}-Cl_{p3}$	1.737 (6)
$C_{b3}-C_{b4}$	1.344 (6)	$C_{p9}-Cl_{p2}$	1.724 (6)	$C_{b11}-C_{b12}$	1.354 (6)	$C_{p19}-Cl_{p4}$	1.718 (7)
Cl_1-O_{11}	1.362 (5)	Cl_1-O_{13}	1.264 (6)	Cl_2-O_{21}	1.350 (10)	Cl_2-O_{24}	1.444 (11)
Cl_1-O_{12}	1.319 (9)	Cl_1-O_{14}	1.346 (5)	Cl_2-O_{22}	1.363 (6)	Cl_2-O_{25}	1.282 (14)
				Cl_2-O_{23}	1.355 (9)	Cl_2-O_{26}	1.416 (20)
						Cl_2-O_{27}	1.227 (12)

[a] The numbers in parentheses are the estimated standard deviations.

$Clpy)_2]ClO_4$. Moreover, it differs significantly from that of the "average" structure of *tri*-$[Fe(OEP)(3\text{-}Clpy)_2]ClO_4$ at 293 K (thermal spin equilibrium structure), even though the magnetic moments of the two phases at this temperature are quite similar. However, the structural pattern observed, "low-spin-like" equatorial bond distances and "high-spin-like" axial bond distances, is that expected[4] for an intermediate-spin iron(III) porphyrinate. The temperature-dependent magnetic susceptibilities are qualitatively in accord with this assignment. Futher evidence for the assignment of an intermediate-spin state to the monoclinic crystal form comes from additional physical characterization.

We have studied both crystalline phases by Mossbauer spectroscopy in the presence and absence of an external magnetic field. The data are listed in Table VIII along with literature data on other iron(III) complexes. In the absence of an applied magnetic field, the spectra of both forms are single quadrupole doublets at all temperatures. (The monoclinic form probably always displays a second doublet attributable to the triclinic form, vide infra.) The Mossbauer data clearly suggest different electronic states for the two crystalline forms of $[Fe(OEP)(3\text{-}Clpy)_2]ClO_4$. The single doublet and lack of a significant temperature dependence on the the Mossbauer parameters of *tri*-$[Fe(OEP)(3\text{-}Clpy)_2]ClO_4$ is somewhat surprising since all other data are consistent with a thermal spin equilibrium; two doublets might have been anticipated. However, a similar lack of quantitative dependence of the Mossbauer parameters in spin crossover systems has been noted previously. This has been attributed to high-spin–low-spin crossover periods shorter than the Mossbauer time scale[17] and to substantial differences in the Debye–Waller factor for the high-spin and low-spin molecules.[18] Apparently some tris(dithiocarbamate) complexes are the only other ferric spin crossover system for which distinct high- and low-spin Mossbauer signals are not seen.[17]

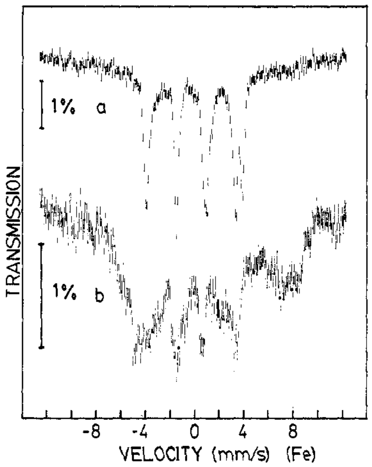

Figure 3. Mossbauer spectra of (a) *mono*- and (b) *tri*-$[Fe(OEP)(3\text{-}Clpy)_2ClO_4$ in a 6-T field at 4.2 K.

The large quadrupole splitting observed for *mono*-$[Fe(OEP)(3\text{-}Clpy)_2]ClO_4$ is generally diagnostic of an intermediate-spin state. The behavior of the samples in an applied magnetic field (6 T) at 4.2 K is quite diagnostic with *tri*-$[Fe(OEP)(3\text{-}Clpy)_2]ClO_4$ displaying a spectrum consistent with an $S = {}^1/_2$

---

(17) Malliaris, A.; Papaefthimiou, V. *Inorg. Chem.* **1982**, *21*, 770–774 and Merithew, P. B.; Rasmussen, P. G. *Ibid.* **1972**, *11*, 325–330 and references therein.

(18) Haddad, M. S.; Lynch, M. W.; Federer, W. D.; Hendrickson, D. N. *Inorg. Chem.* **1981**, *20*, 123–131. Fleisch, J.; Gutlich, P.; Hasselbach, K. M. *Ibid.* **1977**, *16*, 1979–1984 and references cited therein.

species. *mono*-[Fe(OEP)(3-Clpy)$_2$]ClO$_4$ displays a spectrum very similar to those of Fe(TPP)(OClO$_3$)[19] and *Chromatium* cytochrome *c*′[20] which have been assigned quantum-admixed intermediate-spin states. The two spectra are displayed in Figure 3. Finally we note that the Mossbauer spectra of *mono*-[Fe(OEP)(3-Clpy)$_2$]ClO$_4$ can display a second, less intense, quadrupole doublet with isomer shift and quadrupole splitting identical with that of the triclinic phase. The presence and amount of this doublet depends on the previous thermal history of the sample and is interpreted as a thermally induced phase change. Unfortunately, we have been unable to study this in detail owing to a lack of material. However, it appears that the thermally induced phase change was minimized in the Mossbauer studies by rapid cooling of the sample.

The EPR spectrum of solid *mono*-[Fe(OEP)(3-Clpy)$_2$]ClO$_4$ at 77 K has an axial spectrum with $g_\perp = 4.92$ and $g_\parallel = 1.97$. The broad *g* feature is similar to those reported for Fe(TPP)OClO$_3$)[21] and for cytochrome *c*′ from *Chromatium*[22] which have been assigned quantum-admixed intermediate-spin states. The EPR spectrum of the monoclinic phase is quite distinct from that of the triclinic phase which shows weak features characteristic of a high-spin species ($g \approx 6.2$).

We now turn to the interesting questions of the reasons for the formation of the intermediate-spin form[23] of [Fe(OEP)(3-Clpy)$_2$]ClO$_4$ and its apparent stability in the monoclinic phase at ambient temperature and below. We consider first the reasons for retaining the intermediate-spin state in the crystalline (monoclinic) phase.

The previously reported temperature dependence[9a,10,12] of the magnetic moment of [Fe(OEP)(3-Clpy)$_2$]ClO$_4$ suggests that the stable spin state of the molecule at reduced temperature is low spin. Why then does the monoclinic phase not display this electronic state at reduced temperatures? As noted earlier, a significant structural difference between the *tri*- and *mono*-[Fe(OEP)(3-Clpy)$_2$]ClO$_4$ species is the orientation of the 3-chloropyridine ligand plane with respect to the porphinato core. In *tri*-[Fe(OEP)(3-Clpy)$_2$]ClO$_4$, the dihedral angle ϕ between the 3-chloropyridine plane and the coordinate plane containing Fe and two opposite porphinato nitrogen atoms is 41°. This is quite close to the value, 45°, which leads to minimum nonbonded interaction between the porphinato core atoms and axial ligand hydrogen atoms.[24] Thus the orientation of the 3-chloropyridine rings in *tri*-[Fe(OEP)(3-Clpy)$_2$]ClO$_4$ allows a ready contraction of the axial Fe–N(py) bonds (from 2.32 to 2.04 Å) without a significant increase in the steric interaction between the core and the axial ligand. In *mono*-[Fe(OEP)(3-Clpy)$_2$]ClO$_4$, however, the ϕ angles of the four independent 3-chloropyridine ligands are 5.7, 7.0, 11.5, and 13.9°. The relative orientation of the pyridine rings in the two molecules are shown in Figure 4. With the observed long axial bond distances of 2.310 Å, these orientations do not lead to significant nonbonded interaction between pyridine hydrogen atoms and porphinato nitrogen atoms. However, at the Fe–N(py) distance (~2.04 Å) appropriate for a low-spin species, significantly short nonbonded contacts would ensue.[25] Thus the observed orientation of the pyridine rings in *mono*-[Fe(OEP)(3-Clpy)$_2$]ClO$_4$ will resist the structural changes[4] that must accompany a change in spin state to low spin. Moreover, these orientations of the 3-chloropyridine ligand are "locked" in by the packing of the *mono*-[Fe(OEP)(3-Clpy)$_2$]ClO$_4$ molecules in the solid state.[26] Some aspects of the molecular packing will be discussed subsequently. Thus the low-spin state for iron(III) in *mono*-[Fe(OEP)(3-Clpy)$_2$]ClO$_4$ is geometrically disallowed. The equivalence of the solution susceptibilities of *mono*- and *tri*-[Fe(OEP)(3-Clpy)$_2$]ClO$_4$ also points out the importance of solid-state effects on their magnetic properties.

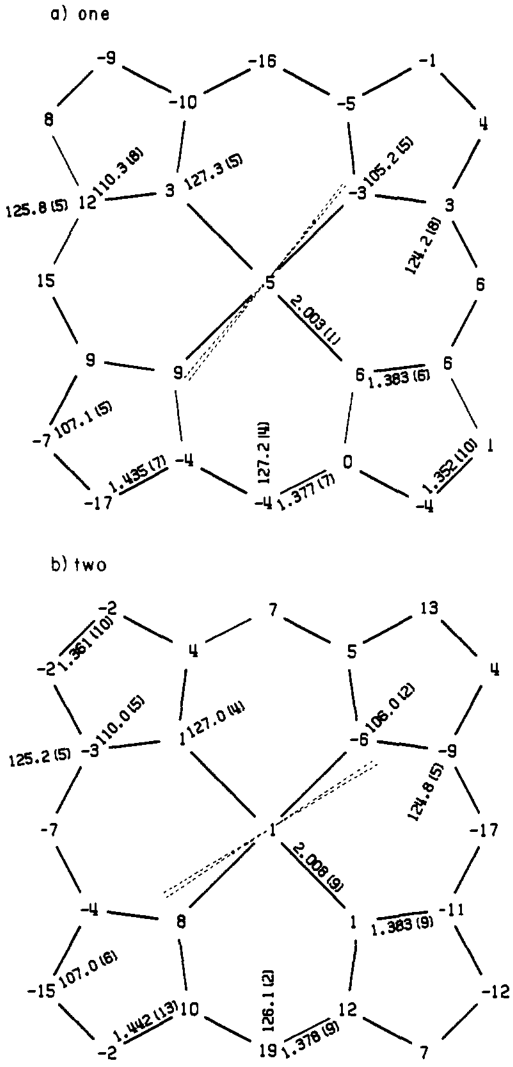

Figure 4. Formal diagrams of the porphinato skeletons in *mono*-[Fe(OEP)(3-Clpy)$_2$]ClO$_4$ showing the relative orientation of the 3-chloropyridine rings (dashed lines) for (a) molecule one and (b) molecule two. The length of the line represents the projection of the ring from the 2-hydrogen to the 5-hydrogen atom positions. The diagrams, which have the same relative orientation as Figures 1 and 2, show the perpendicular displacements of each atom, in units of 0.01 Å, from the mean plane of the 24-atom core. For each molecule, average values of bond distances and angles for each of the chemically distinct classes is displayed.

The foregoing suggests that either a high- or intermediate-spin state is geometrically allowed in the monoclinic phase of [Fe(OEP)(3-Clpy)$_2$]ClO$_4$. The important structural feature common to both states is the long axial bond lengths. Empirical observation[4] demonstrates that the prime determinant of spin state in ferric porphyrinates is the axial ligand field strength. Weak ligand fields favor either high- or intermediate-spin, with the former more frequently observed. Gouterman and Scheidt[27] have performed

---

(19) Spartalian, K.; Lang, G.; Reed, C. A. *J. Chem. Phys.* **1979**, *71*, 1832–1837.

(20) Maltempo, M. M.; Moss, T. H.; Spartalian, K. *J. Chem. Phys.* **1980**, *73*, 2100–2106.

(21) Reed, C. A.; Mashiko, T.; Bentley, S. P.; Kastner, M. E.; Scheidt, W. R.; Spartalian, K.; Lang, G. *J. Am. Chem. Soc.* **1979**, *101*, 2948–2958.

(22) Maltempo, M. M. *J. Chem. Phys.* **1974**, *61*, 2540–2547.

(23) Most, if not all, intermediate-spin porphinatoiron(III) species are properly described as quantum-admixed intermediate-spin species. In this paper, the term intermediate-spin, as applied to *mono*-[Fe(OEP)(3-Clpy)$_2$]ClO$_4$, implies such a quantum-admixed state.

(24) This matter was originally discussed by Hoard. See ref 5.

(25) The average observed H(py)···N(porph) separation in *mono*-[Fe(OEP)(3-Clpy)$_2$]ClO$_4$ is 2.55 Å. This would decrease to ~2.26 Å for the complex in a low-spin (Fe–N(py) ≈ 2.04 Å) configuration. Notably, in the low-spin form of *tri*-[Fe(OEP)(3-Clpy)$_2$]ClO$_4$ with its favorable value of ϕ, the average nonbonded separation is significantly longer at 2.71 Å. The reasons for this are clear from an examination of Figure 4.

(26) Calculation of nonbonded contacts involving the 3-chloropyridine ligands in the observed orientations and assumed orientations (various values of ϕ, including ±45°) reveals unrealistic intermolecular contacts for all assumed configurations but reasonable intermolecular separations (≥3.40 Å) for the observed configuration.

Table VI. Bond Angles in $[Fe(OEP)(3\text{-}Clpy)_2]ClO_4$[a]

angle	degrees	angle	degrees	angle	degrees
A. Molecule One					
$Fe_1N_1C_{a1}$	128.0 (3)	$N_1C_{a2}C_{m2}$	124.3 (1)	$C_{b6}C_{a6}C_{m4}$	125.1 (5)
$Fe_1N_1C_{a2}$	126.6 (3)	$N_2C_{a3}C_{m2}$	124.6 (4)	$C_{b7}C_{a7}C_{m4}$	126.8 (5)
$Fe_1N_2C_{a3}$	126.7 (3)	$N_2C_{a4}C_{m3}$	124.5 (4)	$C_{b8}C_{a8}C_{m1}$	125.4 (4)
$Fe_1N_2C_{a4}$	127.3 (3)	$N_3C_{a5}C_{m3}$	123.6 (4)	$C_{b2}C_{b1}C_{11}$	127.0 (5)
$Fe_1N_3C_{a5}$	127.8 (3)	$N_3C_{a6}C_{m4}$	124.1 (5)	$C_{b1}C_{b2}C_{21}$	128.2 (5)
$Fe_1N_3C_{a6}$	127.1 (3)	$N_4C_{a7}C_{m4}$	123.7 (5)	$C_{b4}C_{b3}C_{31}$	126.9 (5)
$Fe_1N_4C_{a7}$	127.1 (3)	$N_4C_{a8}C_{m1}$	125.4 (4)	$C_{b3}C_{b4}C_{41}$	127.8 (5)
$Fe_1N_4C_{a8}$	127.7 (3)	$C_{a1}N_1C_{a2}$	105.0 (4)	$C_{b6}C_{b5}C_{51}$	127.6 (5)
$Fe_1N_{py1}C_{p1}$	122.0 (3)	$C_{a3}N_2C_{a4}$	105.9 (4)	$C_{b5}C_{b6}C_{61}$	128.6 (5)
$Fe_1N_{py1}C_{p5}$	120.3 (3)	$C_{a5}N_3C_{a6}$	104.9 (4)	$C_{b8}C_{b7}C_{71}$	127.9 (5)
$Fe_1N_{py2}C_{p6}$	121.4 (3)	$C_{a7}N_4C_{a8}$	105.2 (4)	$C_{b7}C_{b8}C_{81}$	128.3 (5)
$Fe_1N_{py2}C_{p10}$	120.7 (3)	$C_{a2}C_{m1}C_{a3}$	126.8 (5)	$C_{b1}C_{11}C_{12}$	112.6 (5)
$N_1Fe_1N_2$	90.5 (1)	$C_{a4}C_{m2}C_{a5}$	126.9 (5)	$C_{b2}C_{21}C_{22}$	112.0 (5)
$N_1Fe_1N_3$	178.8 (2)	$C_{a6}C_{m3}C_{a7}$	127.4 (5)	$C_{b3}C_{31}C_{32}$	114.7 (6)
$N_1Fe_1N_4$	89.7 (1)	$C_{a8}C_{m4}C_{a1}$	127.6 (4)	$C_{b4}C_{41}C_{42}$	114.6 (5)
$N_1Fe_1N_{py1}$	89.2 (1)	$C_{a1}C_{b1}C_{b2}$	106.7 (4)	$C_{b5}C_{51}C_{52}$	119.2 (12)
$N_1Fe_1N_{py2}$	91.7 (2)	$C_{a2}C_{b2}C_{b1}$	107.2 (4)	$C_{b6}C_{61}C_{62}$	111.5 (8)
$N_2Fe_1N_3$	89.7 (2)	$C_{a3}C_{b3}C_{b4}$	107.5 (4)	$C_{b7}C_{71}C_{72}$	95.0 (8)
$N_2Fe_1N_4$	179.6 (2)	$C_{a4}C_{b4}C_{b3}$	107.5 (4)	$C_{b8}C_{81}C_{82}$	114.5 (5)
$N_2Fe_1N_{py1}$	89.3 (1)	$C_{a5}C_{b5}C_{b6}$	106.9 (5)	$C_{p1}N_{py1}C_{p5}$	117.7 (4)
$N_2Fe_1N_{py2}$	89.5 (1)	$C_{a6}C_{b6}C_{b5}$	106.8 (5)	$N_{py1}C_{p1}C_{p2}$	123.2 (5)
$N_3Fe_1N_4$	90.1 (2)	$C_{a7}C_{b7}C_{b8}$	108.0 (5)	$C_{p1}C_{p2}C_{p3}$	118.6 (6)
$N_3Fe_1N_{py1}$	89.6 (1)	$C_{a8}C_{b8}C_{b7}$	106.5 (4)	$C_{p2}C_{p3}C_{p4}$	118.5 (5)
$N_3Fe_1N_{py2}$	89.5 (2)	$C_{a1}C_{b1}C_{11}$	126.3 (4)	$C_{p3}C_{p4}C_{p5}$	120.1 (5)
$N_4Fe_1N_{py1}$	90.3 (1)	$C_{a2}C_{b2}C_{21}$	124.4 (5)	$C_{p3}C_{p4}Cl_{p1}$	120.5 (5)
$N_4Fe_1N_{py2}$	90.8 (1)	$C_{a3}C_{b3}C_{31}$	125.4 (5)	$Cl_{p1}C_{p4}C_{p5}$	119.4 (5)
$N_{py1}Fe_1N_{py2}$	178.6 (1)	$C_{a4}C_{b4}C_{41}$	124.6 (5)	$C_{p4}C_{p5}N_{py1}$	121.9 (5)
$N_1C_{a1}C_{b1}$	111.1 (4)	$C_{a5}C_{b5}C_{51}$	125.5 (5)	$C_{p6}N_{py2}C_{p10}$	117.8 (5)
$N_1C_{a2}C_{b2}$	111.0 (4)	$C_{a6}C_{b6}C_{61}$	124.3 (5)	$N_{py2}C_{p6}C_{p7}$	122.0 (6)
$N_2C_{a3}C_{b3}$	109.3 (4)	$C_{a7}C_{b7}C_{71}$	122.6 (5)	$C_{p6}C_{p7}C_{p8}$	118.9 (6)
$N_2C_{a4}C_{b4}$	109.7 (4)	$C_{a8}C_{b8}C_{81}$	125.2 (5)	$C_{p7}C_{p8}C_{p9}$	119.3 (6)
$N_3C_{a5}C_{b5}$	110.5 (4)	$C_{b1}C_{a1}C_{m1}$	125.8 (4)	$C_{p8}C_{p9}C_{p10}$	119.2 (6)
$N_3C_{a6}C_{b6}$	110.8 (4)	$C_{b2}C_{a2}C_{m2}$	125.7 (5)	$C_{p8}C_{p9}Cl_{p2}$	121.0 (5)
$N_4C_{a7}C_{b7}$	109.5 (4)	$C_{b3}C_{a3}C_{m2}$	126.0 (5)	$Cl_{p2}C_{p9}C_{p10}$	119.8 (5)
$N_4C_{a8}C_{b8}$	110.8 (4)	$C_{b4}C_{a4}C_{m3}$	125.8 (5)	$C_{p9}C_{p10}N_{py2}$	122.7 (5)
$N_1C_{a1}C_{m1}$	123.0 (4)	$C_{b5}C_{a5}C_{m3}$	125.9 (5)	$O_{12}Cl_1O_{14}$	110.0 (6)
$O_{11}Cl_1O_{12}$	107.2 (5)	$O_{11}Cl_1O_{14}$	113.1 (4)	$O_{13}Cl_1O_{14}$	107.6 (5)
$O_{11}Cl_1O_{13}$	113.4 (6)	$O_{12}Cl_1O_{13}$	104.3 (7)		
B. Molecule Two					
$Fe_2N_5C_{a9}$	127.2 (3)	$N_5C_{a10}C_{m6}$	125.2 (5)	$C_{b14}C_{a14}C_{m8}$	125.1 (4)
$Fe_2N_5C_{a10}$	126.6 (3)	$N_6C_{a11}C_{m6}$	124.3 (4)	$C_{b15}C_{a15}C_{m8}$	125.5 (4)
$Fe_2N_6C_{a11}$	127.3 (3)	$N_6C_{a12}C_{m7}$	125.5 (4)	$C_{b16}C_{a16}C_{m5}$	125.4 (4)
$Fe_2N_6C_{a12}$	126.5 (3)	$N_7C_{a13}C_{m7}$	124.2 (4)	$C_{b10}C_{b9}C_{91}$	127.6 (5)
$Fe_2N_7C_{a13}$	126.7 (3)	$N_7C_{a14}C_{m7}$	124.9 (4)	$C_{b9}C_{b10}C_{101}$	127.7 (5)
$Fe_2N_7C_{a14}$	127.3 (3)	$N_8C_{a15}C_{m8}$	124.3 (4)	$C_{b12}C_{b11}C_{111}$	128.0 (5)
$Fe_2N_8C_{a15}$	127.5 (3)	$N_8C_{a16}C_{m5}$	125.2 (4)	$C_{b11}C_{b12}C_{121}$	128.7 (5)
$Fe_2N_8C_{a16}$	126.5 (3)	$C_{a9}N_5C_{a10}$	105.9 (4)	$C_{b14}C_{b13}C_{131}$	127.5 (5)
$Fe_2N_{py3}C_{p11}$	121.9 (3)	$C_{a11}N_6C_{a12}$	106.2 (4)	$C_{b13}C_{b14}C_{141}$	128.9 (5)
$Fe_2N_{py3}C_{p15}$	121.0 (3)	$C_{a13}N_7C_{a14}$	105.7 (4)	$C_{b16}C_{b15}C_{151}$	127.8 (4)
$Fe_2N_{py4}C_{p16}$	122.0 (3)	$C_{a15}N_8C_{a16}$	106.0 (4)	$C_{b15}C_{b16}C_{161}$	127.1 (5)
$Fe_2N_{py4}C_{p20}$	120.7 (3)	$C_{a10}C_{m6}C_{a11}$	126.3 (5)	$C_{b9}C_{91}C_{92}$	110.0 (8)
$N_5Fe_2N_6$	89.9 (2)	$C_{a12}C_{m7}C_{a13}$	126.2 (4)	$C_{b10}C_{101}C_{102}$	111.6 (8)
$N_5Fe_2N_7$	179.6 (2)	$C_{a14}C_{m8}C_{a15}$	126.0 (4)	$C_{b11}C_{111}C_{112}$	112.1 (6)
$N_5Fe_2N_8$	90.0 (2)	$C_{a16}C_{m5}C_{a9}$	126.0 (4)	$C_{b12}C_{121}C_{122}$	117.7 (6)
$N_5Fe_2N_{py3}$	91.8 (2)	$C_{a9}C_{b9}C_{b10}$	106.6 (5)	$C_{b13}C_{131}C_{132}$	111.4 (5)
$N_5Fe_2N_{py4}$	90.0 (2)	$C_{a10}C_{b10}C_{b9}$	106.8 (5)	$C_{b14}C_{141}C_{142}$	112.7 (5)
$N_6Fe_2N_7$	90.5 (1)	$C_{a11}C_{b11}C_{b12}$	106.9 (4)	$C_{b15}C_{151}C_{152}$	114.6 (5)
$N_6Fe_2N_8$	179.7 (1)	$C_{a12}C_{b12}C_{b11}$	107.2 (4)	$C_{b16}C_{161}C_{162}$	113.9 (5)
$N_6Fe_2N_{py3}$	89.1 (1)	$C_{a13}C_{b13}C_{b14}$	107.6 (4)	$C_{p11}N_{py3}C_{p15}$	117.0 (4)
$N_6Fe_2N_{py4}$	89.2 (1)	$C_{a14}C_{b14}C_{b13}$	106.7 (4)	$N_{py3}C_{p11}C_{p12}$	123.2 (5)
$N_7Fe_2N_8$	89.7 (1)	$C_{a15}C_{b15}C_{b16}$	106.4 (4)	$C_{p11}C_{p12}C_{p13}$	119.1 (6)
$N_7Fe_2N_{py3}$	88.5 (1)	$C_{a16}C_{b16}C_{b15}$	108.0 (4)	$C_{p12}C_{p13}C_{p14}$	118.4 (5)
$N_7Fe_2N_{py4}$	89.7 (2)	$C_{a9}C_{b9}C_{91}$	125.7 (5)	$C_{p13}C_{p14}C_{p15}$	120.1 (5)
$N_8Fe_2N_{py3}$	91.2 (1)	$C_{a10}C_{b10}C_{101}$	125.1 (5)	$C_{p13}C_{p14}Cl_{p3}$	120.4 (5)
$N_8Fe_2N_{py4}$	90.6 (1)	$C_{a11}C_{b11}C_{111}$	125.1 (5)	$Cl_{p3}C_{p14}C_{p15}$	119.5 (5)
$N_{py3}Fe_2N_{py4}$	177.5 (1)	$C_{a12}C_{b12}C_{121}$	124.1 (5)	$C_{p14}C_{p15}N_{py3}$	122.2 (5)
$N_5C_{a9}C_{b9}$	110.8 (5)	$C_{a13}C_{b13}C_{131}$	124.7 (5)	$C_{p16}N_{py4}C_{p20}$	117.4 (5)
$N_5C_{a10}C_{b10}$	109.7 (5)	$C_{a14}C_{b14}C_{141}$	124.1 (5)	$N_{py4}C_{p16}C_{p17}$	123.0 (6)
$N_6C_{a11}C_{b11}$	110.3 (4)	$C_{a15}C_{b15}C_{151}$	125.8 (4)	$C_{p16}C_{p17}C_{p18}$	118.8 (6)
$N_6C_{a12}C_{b12}$	109.4 (4)	$C_{a16}C_{b16}C_{161}$	124.9 (4)	$C_{p17}C_{p18}C_{p19}$	118.8 (6)
$N_7C_{a13}C_{b13}$	109.9 (4)	$C_{b9}C_{a9}C_{m5}$	124.4 (4)	$C_{p18}C_{p19}C_{p20}$	118.8 (6)
$N_7C_{a14}C_{b14}$	110.0 (4)	$C_{b10}C_{a10}C_{m6}$	125.0 (5)	$C_{p18}C_{p19}Cl_{p4}$	121.1 (5)
$N_8C_{a15}C_{b15}$	110.2 (4)	$C_{b11}C_{a11}C_{m6}$	125.5 (5)	$Cl_{p4}C_{p19}C_{p20}$	120.1 (6)
$N_8C_{a16}C_{b16}$	109.3 (4)	$C_{b12}C_{a12}C_{m7}$	125.1 (4)	$C_{p19}C_{p20}N_{py4}$	123.2 (6)
$N_5C_{a9}C_{m5}$	124.8 (4)	$C_{b13}C_{a13}C_{m7}$	125.9 (4)	$O_{23}Cl_2O_{27}$	126.8 (12)

Table VI (*Continued*)

angle	degrees	angle	degrees	angle	degrees
$O_{21}Cl_2O_{22}$	117.4 (7)	$O_{22}Cl_2O_{24}$	102.4 (7)	$O_{24}Cl_2O_{25}$	76.7 (11)
$O_{21}Cl_2O_{23}$	107.0 (8)	$O_{22}Cl_2O_{25}$	102.9 (10)	$O_{24}Cl_2O_{26}$	164.8 (9)
$O_{21}Cl_2O_{24}$	102.2 (9)	$O_{22}Cl_2O_{26}$	86.3 (8)	$O_{24}Cl_2O_{27}$	57.9 (9)
$O_{21}Cl_2O_{25}$	138.5 (13)	$O_{22}Cl_2O_{27}$	118.2 (12)	$O_{25}Cl_2O_{26}$	113.8 (13)
$O_{21}Cl_2O_{26}$	62.6 (8)	$O_{23}Cl_2O_{24}$	112.0 (10)	$O_{25}Cl_2O_{27}$	123.8 (12)
$O_{21}Cl_2O_{27}$	44.7 (10)	$O_{23}Cl_2O_{25}$	42.0 (11)	$O_{26}Cl_2O_{27}$	107.0 (11)
$O_{22}Cl_2O_{23}$	115.0 (5)	$O_{23}Cl_2O_{26}$	74.4 (8)		

[a] The numbers in parentheses are the estimated standard deviations.

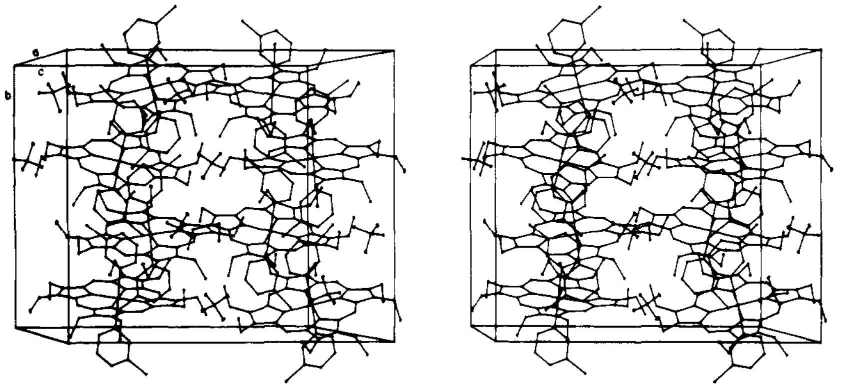

Figure 5. Stereoscopic drawing of the cell contents of *mono*-[Fe(OEP)(3-Clpy)$_2$]ClO$_4$.

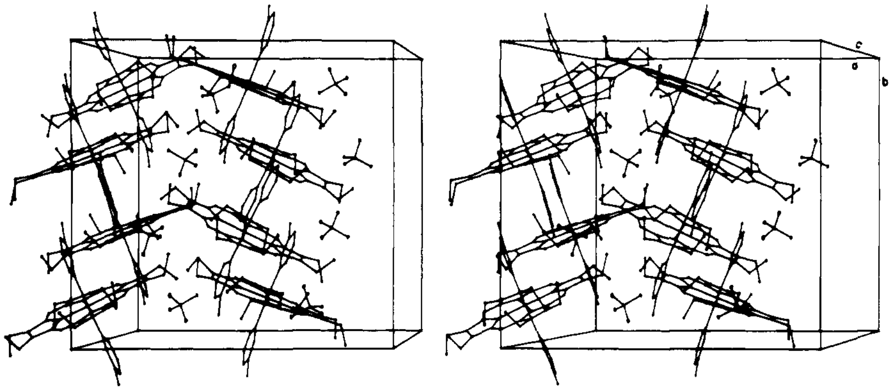

Figure 6. Second stereoscopic view of the unit cell contents of *mono*-[Fe(OEP)(3-Clpy)$_2$]ClO$_4$.

Table VII. Comparison of Coordination Group Distances in *tri*- and *mono*-[Fe(OEP)(3-Clpy)$_2$]ClO$_4$

phase, conditions	Fe-N$_p$[a]	Fe-N(3-Clpy)[a]
triclinic[b]		
low-spin form, 98 K	1.994 (6)	2.031 (2)
"average" structure, 293 K	2.014 (4)	2.194 (2)
low-spin form, 293 K	(1.990)[c]	2.043
high-spin form, 293 K	(2.045)[c]	2.316
monoclinic		
293 K	2.005 (6)	2.310 (17)

[a] The numbers in parentheses are the estimated standard deviations, calculated on the assumption that all averaged values were drawn from the same population. [b] Data from ref 10. [c] Expected value (ref 4), not experimentally determined from the analysis of the thermal spin mixture.

iterative extended Hückel calculations on three six-coordinate porphinato complexes, Fe^{III}(P)L$_2$, where L = CN$^-$, 3-chloropyridine, and H$_2$O, to explore the effect of geometry and ligands on the spin state of iron. These calculations were used to establish relative d orbital energies of each complex in idealized high- and low-spin geometries. A significant conclusion from these calculations was that the electronic energy difference between the $^4A_{2g}$ and $^6A_{2g}$ states will always be small.[28]

Why is the monoclinic phase obtained? In solutions of [Fe(OEP)(3-Clpy)$_2$]ClO$_4$ there is a significant thermal population of species with spin multiplicity greater than $^1/_2$ (probably $S = {}^5/_2$). For this higher multiplicity form of the molecule there should be relatively free rotation about the Fe–N(py) bond. There should thus exist in solution a significant number of molecules having 3-chloropyridine ring orientations of $\phi \approx 0$. We apparently happened upon (for a time) conditions under which the crystal form having molecules with $\phi \approx 0$ was obtained, rather than the (probably more stable) form with $\phi \approx 45°$.[29] Once this rotational isomer of the molecule has been trapped in a crystalline lattice, only the high- or intermediate-spin states are accessible. We can surmise that in these circumstances the intermediate-spin state is energetically more favorable than the high-spin state. This could

---

(27) Scheidt, W. R.; Gouterman, M. In "Physical Bioinorganic Chemistry—Iron Porphyrins, Part I"; Lever, A. B. P., Gray, H. B., Eds.; Addison-Wesley: Reading, MA, 1983; pp 89–139. These calculations were performed before the monoclinic form of [Fe(OEP)(3-Clpy)$_2$]ClO$_4$ had been isolated.

(28) This conclusion derives from the fact that the energy difference between high- and intermediate-spin states is related to the average exchange integral $\bar{K}_{HI}$ and the energy difference between the nearly degenerate d_{xy}, d_{xz}, d_{yz} (t) orbitals and $d_{x^2-y^2}$ (b) with $\Delta E_{HI} = b - t - 4\bar{K}_{HI} \approx 0$. Se ref 27.

(29) A number of equally bizarre and poorly understood crystallization phenomena are known. See Woodard and McCrone (Woodward, G. D.; McCrone, W. C. *J. Appl. Cryst.* **1975**, *8*, 342) for an interesting account.

Table VIII. Mössbauer Parameters of Some Low-, Intermediate-, and High-Spin Ferric Compounds

compound (spin)	T, K	δ,[a] mm s^{-1}	ΔE_q, mm s^{-1}	ref
tri-$[\mathrm{Fe(OEP)(3\text{-}Clpy)_2}]\mathrm{ClO_4}$	4.2	0.28	2.10	
	77	0.28	2.09	
	195	0.27	2.06	
	295	0.27	2.08	this work
mono-$[\mathrm{Fe(OEP)(3\text{-}Clpy)_2}]\mathrm{ClO_4}$	4.2	0.42	2.7	
	77	0.42	2.68	
	195	0.35	2.68	
	295	0.32	2.52	this work
$\mathrm{Fe(TPP)(OClO_3)\cdot 0.5}$*m*-xylene	4.2	0.38	3.50	
(intermediate)	77	0.38	3.48	
	295	0.30	2.79	*b*
$\mathrm{Fe(OEP)(OClO_3)}$	4.2	0.37	3.57	
(intermediate)	295	0.29	3.16	*c*
$\mathrm{Fe(TPP)(C(CN)_3)}$	78	0.30	3.03	
(intermediate)	298	0.30	3.18	*d*
$[\mathrm{Fe(TPP)(Me_2SO)_2}]\mathrm{ClO_4}$ (high spin)	4.2	0.45	1.22	*e*
$[\mathrm{Fe(TPP)(OH_2)_2}]\mathrm{ClO_4}$	78	0.33	1.69	
(high spin)	298	0.41	1.53	*f*
$[\mathrm{Fe(TPP)(py)_2}]\mathrm{Cl}$ (low spin)	77	0.16	1.25	*g*
$[\mathrm{Fe(TPP)(Im)_2}]\mathrm{Cl}$	77	0.23	2.23	
(low spin)	298	0.13	2.11	*g*
$[\mathrm{Fe(PP)(py)_2}]\mathrm{Cl}$ (low spin)	77	0.23	1.88	*g*
$\mathrm{Fe(dtc)_2Cl}$ (intermediate)	77	0.49	2.70	*h*
$\mathrm{Fe(Ph_2[15]N_4)(SPh)}$ (intermediate)	77	0.13	2.55	*i*
Chromatium cytochrome *c'* (intermediate, pH 7.8)	4.2	0.29	2.91	*j*

[a] Relative to metallic iron. [b] Reference 19 and 21. [c] Dolphin, D. H.; Sams, J. R.; Tsin, T. B. *Inorg. Chem.* 1977, *16*, 711-713. [d] Reference 8. [e] Reference 7. [f] Reference 6. [g] Epstein, L. M.; Straub, D. K.; Maricondi, C. *Inorg. Chem.* 1967, *6*, 1720-1725. [h] Chapps, G. E.; McCann, S. W.; Wickman, H. H.; Sherwood, R. C. *J. Chem. Phys.* 1974, *60*, 990-997. [i] Koch, S.; Holm, R. H.; Frankel, R. B. *J. Am. Chem. Soc.* 1975, *97*, 6714–6723. [j] Reference 20.

either be an intrinsic stability or an effect of crystal packing. In either case, the results appear to confirm the conclusion[27] that the energies between the high- and intermediate-spin states is not large. The sensitivity of the spin state of $[\mathrm{Fe(OEP)(3\text{-}Clpy)_2}]\mathrm{ClO_4}$ on environmental factors suggest that protein conformational changes can be a sufficient perturbation to readily modify the spin state of heme. The variation[30] in the amounts of high-, intermediate-, and low-spin species in horseradish peroxidase at various stages of purification is one particularly interesting example of apparent protein conformation effects on the spin state of heme.

The packing of molecules in the unit cell is illustrated in Figures 5 and 6, which are stereo diagrams displaying the unit cell contents. An examination of these figures shows that there is a systematic partial overlap between pyridine rings of adjacent molecules so as to form linear chains of molecules more or less parallel to the *b* axis. A given chain is comprised of the two independent molecules in the asymmetric unit and molecules translated along the *b* direction. The partially overlapped pyridine rings are almost parallel; the dihedral angles between the pairs of rings are 3.5° and 4.1°. The average separation between thee planes of the pyridine rings is 3.45 Å. The porphyrin planes along the chain are also almost parallel; the dihedral angle is 8.1° and the interplanar separation is 9.2 Å. This leads to the shortest Fe···Fe separation in the lattice of 9.88 Å. Other Fe···Fe distances range from 10.02 Å upward.

Figure 4 present formal diagrams of the two porphinato cores and displays the perpendicular displacements, in units of 0.01 Å, of each atom from the mean plane of the 24-atom core. The deviations from exact planarity, although significant, are unremarkable for porphinato species. For molecule one, although the iron(III) atom is displaced 0.05 Å from the 24-atom mean plane, the displacement from the plane of the four porphinato nitrogen atoms is less than 0.01 Å. Thus the two iron atoms are virtually centered in their respective porphinato planes. Figure 4 also presents the average values for the chemically distinct bond distances and angles for each molecule. The numbers in parentheses for these averaged values are the estimated standard deviations calculated on the assumption that the values are drawn from the same population. The four independent pyridine planes, including the 3-chloro substituent, are all planar to within 0.01 Å.

Conclusion

The $[\mathrm{Fe(OEP)(3\text{-}Clpy)_2}]\mathrm{ClO_4}$ system, which was originally described as a thermal spin equilibrium ($S = {}^5/_2 \rightleftarrows S = {}^1/_2$) system, has been found to be more complex. Under solid-state conditions, a quantum-admixed ($S = {}^3/_2, {}^5/_2$) intermediate-spin state can be stabilized. Thus the complex $[\mathrm{Fe(OEP)(3\text{-}Clpy)_2}]\mathrm{ClO_4}$ can be, in principle, manipulated by thermal and/or solid-state effects into displaying three distinct spin states. This suggests that for at least one heme system all three possible spin states can be relatively close in energy.

Acknowledgment. We thank the National Institutes of Health for support of this work under Grants HL-15627 (W.R.S) and HL-16860 (G.L.). We are grateful to Professors P. G. Rasmussen and Larry Garber for access to magnetic susceptibility apparatus. W.R.S. acknowledges the hospitality of and stimulating discussions on electronic properties of hemes with Prof. Martin Gouterman during a sabbatical leave at the University of Washington.

Registry No. $[\mathrm{Fe(OEP)(3\text{-}Clpy)_2}]\mathrm{ClO_4}$, 71414-31-8.

Supplementary Material Available: Table III, final anisotropic temperature factors, Table IV, a listing of the fixed hydrogen atom positions, and a listing of the observed and calculated structure amplitudes (X10) for *mono*-$[\mathrm{Fe(OEP)(3\text{-}Clpy)_2}]\mathrm{ClO_4}$ (47 pages). Ordering information is given on any current masthead page.

---

(30) Maltempo, M. M.; Ohlsson, P.-I.; Paul, K.-G.; Petersson, L.; Ehrenberg, A. *Biochemistry* **1979**, *18*, 2935-2941.